INTERNATIONAL JOURNAL FOR NUMERICAL METHODS IN FLUIDS
Int. J. Numer. Meth. Fluids 2007; **53**:1077–1105
Published online 22 September 2006 in Wiley InterScience (www.interscience.wiley.com). DOI: 10.1002/fld.1356

Implementation of CLEAR algorithm on non-orthogonal curvilinear co-ordinates for solution of incompressible flow and heat transfer

Z. G. Qu, Y. L. He, C. Y. Zhao and W. Q. Tao*, †

State Key Laboratory of Multiphase Flow in Power Engineering, School of Energy and Power Engineering, Xi'an Jiaotong University, Xi'an, Shaanxi 710049, People's Republic of China

SUMMARY

In this paper, the CLEAR (coupled and linked equations algorithm revised) algorithm is extended to non-orthogonal curvilinear collocated grids. The CLEAR algorithm does not introduce pressure correction in order to obtain an incompressible flow field which satisfies the mass conservation law. Rather, it improves the intermediate velocity by solving an improved pressure equation to make the algorithm fully implicit since there is no term omitted in the derivation process. In the extension of CLEAR algorithm from a staggered grid system in Cartesian coordinates to collocated grids in non-orthogonal curvilinear coordinates, three important issues are appropriately treated so that the extended CLEAR can lead to a unique solution without oscillation of pressure field and with high robustness. These three issues are (1) solution independency on the under-relaxation factor; (2) strong coupling between velocity and pressure; and (3) treatment of the cross pressure gradient terms. The flow and heat transfer problems in a rectangular enclosure with an internal eccentric circle and the flow in a lid-driven inclined cavity are computed by using the extended CLEAR. The results show that the extended CLEAR can guarantee the solution independency on the under-relaxation factor, the smoothness of pressure profile even at very small under-relaxation factor and good robustness which leads to a converged solution for the small inclined angle of 5° only with 5-point computational molecule while the extended SIMPLE-series algorithm usually can get a converged solution for the inclined angle larger than 30° under the same condition. Copyright © 2006 John Wiley & Sons, Ltd.

Received 21 December 2005; Revised 30 June 2006; Accepted 6 July 2006

KEY WORDS: CLEAR algorithm; non-orthogonal curvilinear coordinates; incompressible flow; heat transfer

*Correspondence to: W. Q. Tao, State Key Laboratory of Multiphase Flow in Power Engineering, School of Energy and Power Engineering, Xi'an Jiaotong University, Xi'an, Shaanxi 710049, People's Republic of China.
†E-mail: wqtao@mail.xjtu.edu.cn

Contract/grant sponsor: National Natural Science Foundation of China; contract/grant numbers: 50476046, 50425620, 50576069
Contract/grant sponsor: Basic Research Program of China; contract/grant number: 2006CB601203

INTRODUCTION

For numerical simulation of incompressible fluid flow and convective heat transfer problems in complex geometries, non-orthogonal, body fitted coordinates are often adopted in which governing equations are converted from the physical domain to the computational domain. In this case, the collocated grid system [1, 2] is usually applied for the convenience of the code development.

As far as the velocity and pressure coupling algorithm is concerned, extensions of the SIMPLE series algorithm to non-staggered grids in non-orthogonal coordinates are widely used. The SIMPLE algorithm was first proposed by Patankar and Spalding [3] in 1972. It is then modified to several variants to enhance its convergence rate, and References [4–11] may be consulted for the details. Moukalled and Darwish [12] made a comprehensive review and given a unified reorganized expression for all the SIMPLE-like pressure correction algorithms. The common feature of these algorithms is to introduce a pressure correction term and neglect the effect of pressure corrections of neighbouring points. Hence, all these variants are semi-implicit in nature [13]. This assumption will not affect the final solutions when the iterative process converges [14], but does affect the convergence rate as described in Reference [15].

The present authors proposed a fully implicit segregated algorithm CLEAR (coupled and linked equations algorithm revised) for incompressible fluid flow and heat transfer [16, 17]. The CLEAR algorithm discards the basic assumption of the SIMPLE series algorithm to improve the convergence rate and robustness. Recently, the CLEAR algorithm has been extended to orthogonal collocated grid coordinates in Reference [18].

In the development of the numerical methods for the non-staggered grids in non-orthogonal coordinates, the SIMPLE-like algorithms have been extended. These include the SIMPLE, SIMPLER, SIMPLEM algorithm [19] and PISO [20]. When extending an algorithm from the staggered grids in orthogonal coordinates to the non-staggered grids in non-orthogonal coordinates, some new issues occur which should be appropriately dealt with in order to have good convergence and robustness. The first issue is the choice of the dependent variables and the face velocity. Shyy and Vu [21] indicated that a good combination is to use the Cartesian velocity components as the primary variables and the contravariant velocity as cell face velocity, which can satisfy different conservation laws. This choice has been widely accepted in the literatures, and thus is the present paper.

The second issue is the effect of the under-relaxation factor on the velocity solutions. In order to prevent the unphysical pressure oscillation in the non-staggered grid the so-called momentum interpolation (MIM) for the interface velocity proposed in References [1, 2] is widely adopted. However, it is revealed in Reference [22] that in the MIM proposed in References [1, 2] when the under-relaxation of velocity is incorporated into the solution procedure, the final expression for the interface velocity is actually a combination of MIM and linear interpolation. This leads to some dependence of the velocity solution on the under-relaxation factor. Several methods [23–27] have been proposed to overcome this undesirable feature of MIM among whom is the SIMPLES proposed in Reference [23]. The SIMPLES [23] algorithm sets the under-relaxation factor $\alpha = 1$ before the momentum interpolation is implemented, but this practice may decrease the robustness of the algorithm to some extent. Choi *et al*. [27] proposed a calculation procedure of SIMPLE algorithm to eliminate the effect of under-relaxation factor and avoid the additional correction term. It was found that if the contravariant velocity was selected as cell face velocity, the unstable convergence history might occur when the grid non-orthogonality was significant, so the covariant velocity components were chosen as the cell-face velocities. However, using the covariant velocity

DOI: 10.1002/fld

Table I. Algorithms comparison.

	Under-relaxation factor considered	Cell face being contravariant velocity	Pressure predicted	Neighbouring velocities considered	Non-orthogonal terms considered
Rhie–Chow [1]	N	Y	N	N	N
Extended SIMPLER [19]	N	Y	Y	N	N
SIMPLEM [19]	N	Y	N	Y	Y
Choi and Nam [27]	Y	N	Y	N	N
Extended CLEAR	Y	Y	Y	Y	Y

components as cell face velocities will not fully guarantee the geometric conservation law in the discrete form as indicated in Reference [21].

The third numerical issue is related to the pressure correction equation. In the derivation of the pressure correction equation in the non-orthogonal coordinates, the effects of neighbouring velocities corrections and the non-orthogonal terms are often neglected in order to get a 5-point computational molecule for 2D case and 7-point molecule for 3D case, otherwise the pressure correction equation will be of 9-point computational molecule for 2D case and 19-point for 3D case. Peric [28] pointed out that if the practice of neglecting non-orthogonal term is adopted, the SIMPLE algorithm will exhibit poor convergence behaviour when the intersection angle between gird lines is less than 45° and fail to converge when the angle is below 30°.

The final issue is related to the another weakness of the MIM of References [1, 2]. It has been shown in Reference [29] if the original MIM proposed in References [1, 2] is used, the predicted pressure field may still exhibit oscillations when the under-relaxation factor is quite small.

From the above brief review, it can be seen that up-to now the variety of the extensions of the SIMPLE series algorithm in the non-orthogonal non-staggered grid system often possesses some weaknesses (under-relaxation factor dependence, poor robustness, and possible oscillation of predicted pressure field). This situation motivates the present authors to extend the CLEAR algorithm to the non-orthogonal, non-staggered grid system to discard the above-mentioned undesirable features. The characteristics of the above major algorithm are compared with CLEAR algorithm in Table I. From the table it can be seen that even though all the issues have been addressed individually in this or that way, but it seems to the present authors that so far no algorithm could deal with all the issues successfully.

In this study, the CLEAR algorithm is extended to non-orthogonal curvilinear collocated grids. With careful and appropriate treatments of the above issues, we succeed in construction of an extended CLEAR whose robustness, convergence performance and the solution uniqueness have been greatly improved. For example when an extended SIMPLER algorithm is used, the smallest oblique angle for obtaining a converged solution of the flow in a lid-driven inclined cavity is limited to 30°, while with the extended CLEAR algorithm this angle can reach as small as 5°. For the clarity of presentation, the algorithm which can be adopted in the non-orthogonal, curvilinear, non-staggered grid system will hereafter be called ‘extended’, for example, extended SIMPLER, so that it can be differentiated from its original version in the physical space with staggered grid.

The CLEAR algorithm belongs to the category of segregated approaches. On a non-orthogonal non-staggered grid system its implementation includes three steps: predictor step, intermediate

DOI: 10.1002/fld

step and corrector step. In the following, the mathematical formulation of the extended SIMPLE algorithm is briefly reviewed, then the extended CLEAR algorithm is formulated and finally some numerical examples are conducted to verify the feasibility of the proposed algorithm.

GOVERNING EQUATIONS AND DISCRETIZATION

In order to simplify the formulation, an incompressible steady-state fluid flow and heat transfer in two dimensions is taken as example. For the two-dimensional Cartesian coordinates, the governing equations in the physical domain can be expressed as

$$\frac{\partial(\rho u\phi)}{\partial x}+\frac{\partial(\rho v\phi)}{\partial y}=\frac{\partial}{\partial x}\left(\Gamma\frac{\partial\phi}{\partial x}\right)+\frac{\partial}{\partial y}\left(\Gamma\frac{\partial\phi}{\partial y}\right)+R(x,y) \tag{1}$$

where ϕ is the general dependent variable, $R(x, y)$ is the source term (see Table II). The two curvilinear coordinates ξ, η are introduced, and their relation with the two independent variables of Cartesian coordinates is as follows:

$$x=x(\xi,\eta) \tag{2}$$

$$y=y(\xi,\eta) \tag{3}$$

Based on Equations (2) and (3), the governing equation is converted from the physical domain to the computational domain:

$$\frac{1}{J}\frac{\partial(\rho U\phi)}{\partial\xi}+\frac{1}{J}\frac{\partial(\rho V\phi)}{\partial\eta}=\frac{1}{J}\frac{\partial}{\partial\xi}\left[\frac{\Gamma}{J}(\alpha\phi_\xi-\beta\phi_\eta)\right]+\frac{1}{J}\frac{\partial}{\partial\eta}\left[\frac{\Gamma}{J}(-\beta\phi_\xi+\gamma\phi_\eta)\right]+S(\xi,\eta) \tag{4}$$

In Equation (4), the parameter α, β, γ and J are geometry factors and U, V are named contravariant velocity components. They are defined as

$$\alpha=x_\eta^2+y_\eta^2,\quad \beta=x_\xi x_\eta+y_\xi y_\eta,\quad \gamma=x_\xi^2+y_\xi^2,\quad J=x_\xi y_\eta-x_\eta y_\xi \tag{5}$$

$$U=uy_\eta-vx_\eta \tag{6a}$$

$$V=vy_\xi-ux_\xi \tag{6b}$$

Table II. Values of ϕ, Γ_ϕ and R_ϕ.

ϕ	Γ	R
u	η	$-\frac{\partial p}{\partial x}$
v	η	$-\frac{\partial p}{\partial y}$
T	$\frac{\mu}{\mathrm{Pr}}$	0

DOI: 10.1002/fld

The source terms for $u$and v components can be expressed as

$$\frac{\partial p}{\partial x} = \frac{1}{J}(y_\eta \phi_\xi - y_\eta \phi_\eta) \tag{7}$$

$$\frac{\partial p}{\partial y} = \frac{1}{J}(-x_\eta \phi_\xi - x_\xi \phi_\eta) \tag{8}$$

The control volumes in the physical domain and computational domain are shown in Figures 1 and 2, respectively. In collocated grid system, the main nodes are just grids points of control volumes where the variable to be solved are located and we called these variables main node variables. On the other hand, the contravariant velocity components are located in the interfaces to help to calculate the discretized equations coefficients. The governing equations are discretized with the finite volume method (FVM) [13, 30]. The final discretized results are expressed as follows:

Continuity equation:

$$(\rho \Delta\eta U_f)_e - (\rho \Delta\eta U_f)_w + (\rho \Delta\xi V_f)_n - (\rho \Delta\xi V_f)_s = 0 \tag{9}$$

where U_f, V_f stand for the interface contravariant velocities which are interpolated from the values of the neighbouring nodes.

Momentum equations in which the under-relaxation factor is incorporated:

$$\frac{A_P^u}{\alpha_u} u_P = \sum A_{\mathrm{nb}}^u u_{\mathrm{nb}} - B_P^u \frac{\partial p}{\partial \xi} - C_P^u \frac{\partial p}{\partial \eta} + b^u + \frac{1-\alpha_u}{\alpha_u} A_P^u u_P^0 \tag{10}$$

$$\frac{A_P^v}{\alpha_v} v_P = \sum A_{\mathrm{nb}}^v v_{\mathrm{nb}} - B_P^v \frac{\partial p}{\partial \xi} - C_P^v \frac{\partial p}{\partial \eta} + b^v + \frac{1-\alpha_v}{\alpha_v} A_P^v v_P^0 \tag{11}$$

The pressure gradient terms for u and v equations are discretized in the following expressions:

$$\frac{\partial p}{\partial \xi} = \frac{(p_e)_P - (p_w)_P}{\Delta\xi} \tag{12}$$

$$\frac{\partial p}{\partial \eta} = \frac{(p_n)_P - (p_s)_P}{\Delta\eta} \tag{13}$$

where the interface pressure $(p_e)_P$, $(p_w)_P$, $(p_n)_P$, $(p_s)_P$ are linearly interpolated from the neighbouring nodes.

The coefficients of the discretized equations (10), (11) are calculated as follows:

$$B_P^u = \left(\frac{\partial y}{\partial \eta}\right)_P \Delta\xi\Delta\eta, \quad C_P^u = -\left(\frac{\partial y}{\partial \xi}\right)_P \Delta\xi\Delta\eta \tag{14}$$

$$B_P^v = -\left(\frac{\partial x}{\partial \eta}\right)_P \Delta\xi\Delta\eta, \quad C_P^v = \left(\frac{\partial x}{\partial \xi}\right)_P \Delta\xi\Delta\eta \tag{15}$$

$$A_E = D_e A(|P_{\Delta e}|) + [\![-F_e, 0]\!], \quad A_W = D_w A(|P_{\Delta w}|) - [\![F_w, 0]\!] \tag{16a}$$

DOI: 10.1002/fld

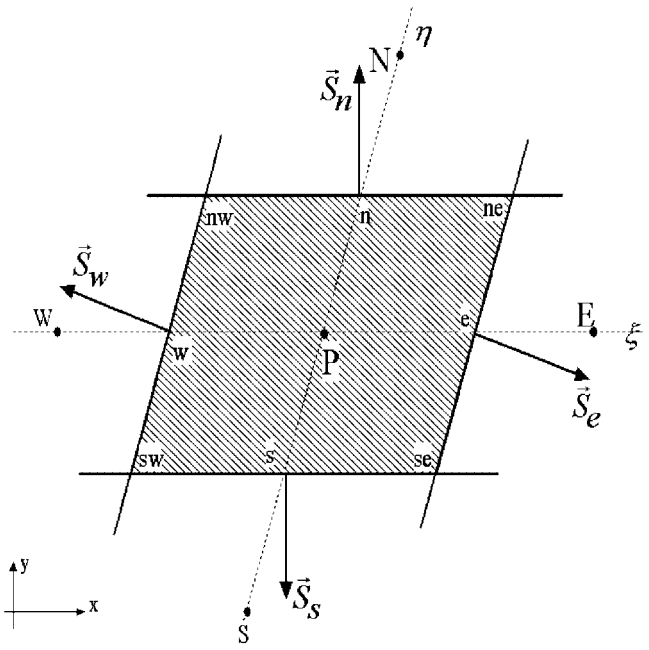

Figure 1. Control volume in the curvilinear coordinates.

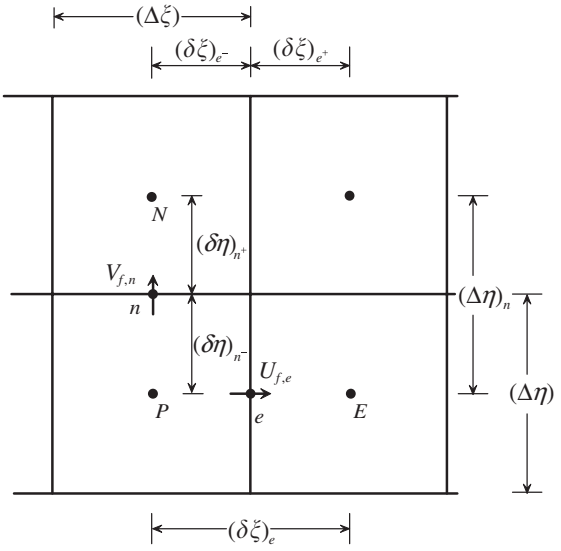

Figure 2. The geometry factor in the computational domain.

DOI: 10.1002/fld

$$A_N = D_n A(|P_{\Delta n}|) + [\![-F_n, 0]\!], \quad A_S = D_s A(|P_{\Delta s}|) - [\![F_s, 0]\!] \tag{16b}$$

$$A_P = A_E + A_W + A_N + A_S \tag{17}$$

$$b^u = SJ\Delta\xi\Delta\eta - \left[\left(\frac{\Gamma}{J}\beta u_\eta \Delta\eta\right)\Big|_w^e + \left(\frac{\Gamma}{J}\beta u_\xi \Delta\xi\right)\Big|_s^n\right] \tag{18a}$$

$$b^v = SJ\Delta\xi\Delta\eta - \left[\left(\frac{\Gamma}{J}\beta v_\eta \Delta\eta\right)\Big|_w^e + \left(\frac{\Gamma}{J}\beta v_\xi \Delta\xi\right)\Big|_s^n\right] \tag{18b}$$

In Equation (16), F and D are flow rate and diffusion conductivity:

$$F_e = (\rho U \Delta\eta)_e, \quad F_w = (\rho U \Delta\eta)_w \tag{19a}$$

$$F_e = (\rho V \Delta\xi)_e, \quad F_w = (\rho V \Delta\xi)_w \tag{19b}$$

$$D_e = \left(\frac{\alpha}{J}\Gamma\frac{\Delta\eta}{\Delta\xi}\right)_e, \quad D_w = \left(\frac{\alpha}{J}\Gamma\frac{\Delta\eta}{\Delta\xi}\right)_w \tag{20a}$$

$$D_n = \left(\frac{\gamma}{J}\Gamma\frac{\Delta\xi}{\Delta\eta}\right)_n, \quad D_s = \left(\frac{\gamma}{J}\Gamma\frac{\Delta\xi}{\Delta\eta}\right)_s \tag{20b}$$

In the above presentation the discretization of the general diffusion–convection equation and the mass conservation equation on the collocated grid have been presented. The solution of the resulting algebraic equations is done usually in segregated manner. Since for incompressible flow pressure does not have its own governing equation, some specially designed method must be adopted in order to correct the intermediately up-dated velocities such that the mass conservation condition can be satisfied at any iteration level. In this regard, the so-called algorithm issue is involved. In the following the extended-SIMPLER algorithm proposed by Acharya *et al.* [19] will first be briefly introduced, then the extended CLEAR algorithm will be presented in detail.

BRIEF REVIEW OF THE EXTENDED SIMPLER ALGORITHM OF ACHARYA *ET AL.* [19]

Some major steps in the development of the extended SIMPLER algorithm proposed in Reference [19] are briefly introduced here just for the comparison with the extended CLEAR algorithm which will be presented in the next section. For the clarity of presentation, the algorithm is presented in two steps: predictor step and corrector step. For the simplicity of presentation only those contents related to the characters of the algorithm will be presented. For the details of the development, Reference [19] should be consulted.

Predictor step of extended SIMPLER algorithm

In this step the pressure equation is formulated. The derivation procedure is similar to the conventional SIMPLER algorithm , hence the details are omitted here. Only the following features should be pointed out: (1) when the momentum discretized equations, Equations (10) and (11) are used to finally construct the interface contravariant velocity, the under-relaxation factor is resumed

DOI: 10.1002/fld

to 1; (2) the cross gradient term of pressure appeared in Equations (10) and (11) are explicitly taken into account.

With the pressure values solved from the above derived pressure equation at hand the discretized momentum equations can be solved, and intermediate up-dated velocities (u_P^*, v_P^*) are obtained. This is done in the corrector step.

Corrector step of extended SIMPLER algorithm

The interface Cartesian velocities are linearly interpolated from the values at the main nodes after solving the momentum equations:

$$u_e^* = \frac{(\delta\xi)_{e^-}}{(\delta\xi)_e} u_E^* + \frac{(\delta\xi)_{e^+}}{(\delta\xi)_e} u_p^*, \quad v_e^* = \frac{(\delta\xi)_{e^-}}{(\delta\xi)_e} v_E^* + \frac{(\delta\xi)_{e^+}}{(\delta\xi)_e} v_P^* \tag{21a}$$

$$v_n^* = \frac{(\delta\eta)_{n^-}}{(\delta\eta)_n} v_N^* + \frac{(\delta\eta)_{n^+}}{(\delta\eta)_n} v_P^*, \quad u_n^* = \frac{(\delta\eta)_{n^-}}{(\delta\eta)_n} u_N^* + \frac{(\delta\eta)_{n^+}}{(\delta\eta)_n} u_P^* \tag{21b}$$

The corresponding contravariant velocities are calculated from Equations (32a) and (32b):

$$\overline{U_e^*} = \left(u^* \frac{\partial y}{\partial \eta} - v^* \frac{\partial x}{\partial \eta} \right)_e = u_e^* (y_\eta)_e - v_e^* (x_\eta)_e \tag{22a}$$

$$\overline{V_n^*} = \left(v^* \frac{\partial x}{\partial \xi} - u^* \frac{\partial y}{\partial \xi} \right)_n = v_n^* (x_\xi)_n - u_n^* (y_\xi)_n \tag{22b}$$

In Reference [19] for preventing the checkerboard pressure distribution in the non-staggered grids, an additional pressure gradient term is added to the right end of Equations (22a) and (22b). The final cell interface velocities are then expressed as

$$U_e^* = \overline{U_e^*} - B_{fe}^{0u} \left(\frac{p_E - p_P}{\Delta\xi} - \overline{p}_\xi \right) \tag{23a}$$

$$V_n^* = \overline{V_n^*} - C_{fn}^{0v} \left(\frac{p_N - p_P}{\Delta\eta} - \overline{p}_\eta \right) \tag{23b}$$

where B_{fe}^{0u}, C_{fn}^{0v} are some coefficients whose expressions can be found in Reference [19].

The term $[(p_N - p_P)/\Delta\eta] - \overline{p}_\eta)$ in Equation (23b) is the referred additional term, $\overline{p}_\xi$, $\overline{p}_\eta$ is the average pressure gradient in the ξ and η directions for the studied control volume, respectively. When the pressure field oscillation occurs it will lead to dissatisfaction of mass conservation and, hence, in the next iteration such oscillating pressure distribution will gradually be smoothed [19].

The above cell interface velocities may not satisfy the mass conservation condition, and the pressure correction equation is formulated for seeking a pressure correction term. With this pressure correction term corresponding velocity correction terms can be obtained. The requirement for the velocity terms is that the intermediate velocities plus their corresponding correction terms should satisfy the mass conservation law. Similar to the derivation of SIMPLER algorithm in the staggered

DOI: 10.1002/fld

grid system [4], such velocity correction terms are:

$$u'_P = \sum A^{0u}_{\mathrm{nb}} u'_{\mathrm{nb}} - B^0_{uP} \frac{\partial p'}{\partial \xi} - C^0_{uP} \frac{\partial p'}{\partial \eta} \tag{24a}$$

$$v'_P = \sum A^{0v}_{\mathrm{nb}} v'_{\mathrm{nb}} - B^0_{vP} \frac{\partial p'}{\partial \xi} - C^0_{vP} \frac{\partial p'}{\partial \eta} \tag{24b}$$

In order to make the derived equations for u'_P, v'_P manageable, the velocity correction terms of the neighbouring grid points $\sum A^{0u}_{\mathrm{nb}} u'_{\mathrm{nb}}$ and $\sum A^{0v}_{\mathrm{nb}} v'_{\mathrm{nb}}$ should be omitted, which is one of the essential character of SIMPLE series algorithm. After such simplification, the velocity correction terms for u and v at the main grids are expressed as

$$u'_P = -B^0_{uP} \frac{\partial p'}{\partial \xi} - C^0_{uP} \frac{\partial p'}{\partial \eta} \tag{24c}$$

$$v'_P = -B^0_{vP} \frac{\partial p'}{\partial \xi} - C^0_{vP} \frac{\partial p'}{\partial \eta} \tag{24d}$$

The improved velocities at main node are then:

$$u_P = u^*_p + u'_P \tag{25a}$$

$$v_P = v^*_p + v'_P \tag{25b}$$

The intermediate contravariant velocities at main node are:

$$U_P = \left(u^* \frac{\partial y}{\partial \eta} - v^* \frac{\partial x}{\partial \eta} \right)_P \tag{26a}$$

$$V_P = \left(v^* \frac{\partial x}{\partial \xi} - u^* \frac{\partial y}{\partial \xi} \right)_P \tag{26b}$$

From Equations (26a) and (26b) the following equations for contravariant velocity corrections at main nodes can be obtained:

$$U'_P = (u' y_\eta - v' x_\eta)_P, \quad V'_P = (v' x_\xi - u' y_\xi)_P \tag{27}$$

By substituting Equations (24a), (24b) into Equation (27) and re-organizing the terms. We can arrive to

$$U'_P = (-y_\eta B^0_{uP} + x_\eta B^0_{vP}) p'_\xi + (-y_\eta C^0_{uP} + x_\eta C^0_{vP}) p'_\eta \tag{28a}$$

$$V'_P = (-x_\xi C^0_{vP} + y_\xi C^0_{uP}) p'_\eta + (-x_\xi B^0_{vP} + y_\xi B^0_{uP}) p'_\xi \tag{28b}$$

To obtain a 5-point molecule for the pressure corrections equations of two-dimensional cases, the cross pressure gradient terms are omitted and the final contravariant velocity corrections at the

DOI: 10.1002/fld

main node are expressed as

$$U'_P = (-y_\eta B^0_{uP} + x_\eta B^0_{vP}) p'_\xi \tag{29a}$$

$$V'_P = (-x_\xi C^0_{vP} + y_\xi C^0_{uP}) p'_\eta \tag{29b}$$

As indicated in Reference [28] with this simplification, the algorithm will have poor convergence behaviour when the angle between grid lines is less than 45°. By mimicking Equations (29a) and (29b), the cell contravariant velocities are obtained.

$$U'_e = -B^{0u}_{fe} p'_\xi, \quad V'_n = -C^{0v}_{fn} p'_\eta \tag{30}$$

where

$$B^{0u}_{fe} = \left(\frac{y^2_\eta \alpha_u}{A^{0u}_P} + \frac{x^2_\eta \alpha_v}{A^{0v}_P} \right)_e (\delta\xi)_e \Delta\eta \tag{31a}$$

$$C^{0v}_{fn} = \left(\frac{x^2_\xi \alpha_v}{A^{0v}_P} + \frac{y^2_\xi \alpha_u}{A^{0u}_P} \right)_n (\delta\eta)_n \Delta\xi \tag{31b}$$

The revised contravariant interface velocity can be expressed as

$$U_e = U^*_e - \left(B^{0u}_f \frac{\partial p'}{\partial \xi} \right)_e \tag{32a}$$

$$V_n = V^*_n - \left(C^{0v}_f \frac{\partial p'}{\partial \eta} \right)_n \tag{32b}$$

It is required that U_e and V_n satisfy the continuity equation. Equations (32a) and (32b) are substituted into the continuity equation, and the pressure correction equation is obtained:

$$A^0_P p'_p = \sum A^0_{\mathrm{nb}} p'_{\mathrm{nb}} + b \tag{33}$$

and the improved pressure is

$$p = p^* + p' \tag{34}$$

From the above brief review for the extended SIMPLER algorithm proposed in Reference [19], the following three aspects should be noted: (1) the presence of the under-relaxation factor is not considered; (2) the additional pressure gradient term is introduced to the interface velocity in the *correction* step; (3) the effects of neighbouring velocity corrections and the cross pressure gradient terms are dropped in the corrector step. These features may affect the performance of the algorithm greatly. In the CLEAR algorithm, however, all these undesirable aspects are discarded.

MATHEMATICAL FORMULATION OF EXTENDED CLEAR ALGORITHM

The CLEAR algorithm is a fully implicit algorithm which does not introduce the correction terms for pressure and velocity as in the SIMPLE series algorithm. Rather, it solves the improved pressure

DOI: 10.1002/fld

directly. Since the intermediate velocities for the neighbouring grid points can be used, no any term is dropped in the derivation of the improved pressure equation. In this sense the effects of the neighbouring grid velocities are fully taken into account. In the orthogonal, staggered and collocated grid system, CLEAR algorithm exhibits very good behaviour [16–18].

In the following the CLEAR algorithm is extended to the non-staggered grid system in non-orthogonal curvilinear coordinates.

Predictor step of extended CLEAR algorithm

Equations (10), (11) are re-written in the explicit manner:

$$u_P = \widehat{u_P^0} - B_{uP}^0 \left(\frac{\partial p}{\partial \xi}\right)_P - C_{uP}^0 \left(\frac{\partial p}{\partial \eta}\right)_P + (1-\alpha_u)u_p^0 \tag{35a}$$

$$v_P = \widehat{v_P^0} - B_{vP}^0 \left(\frac{\partial p}{\partial \xi}\right)_P - C_{vP}^0 \left(\frac{\partial p}{\partial \eta}\right)_P + (1-\alpha_v)v_p^0 \tag{35b}$$

where the pseudo-velocity $\widehat{u_P^0}$ and $\widehat{v_P^0}$ and the coefficients are calculated as follows:

$$\widehat{u_P^0} = \frac{\sum A_{\mathrm{nb}}^{0u} u_{\mathrm{nb}}^0 + b_P^{0u}}{(A_P^{0u})_P/\alpha_u} \tag{36a}$$

$$\widehat{v_P^0} = \frac{\sum A_{\mathrm{nb}}^{0v} v_{\mathrm{nb}}^0 + b_P^{0v}}{(A_P^{0v})_P/\alpha_v} \tag{36b}$$

$$b_P^{0u} = SJ\Delta\xi\Delta\eta - \left[\left(\frac{\Gamma}{J}\beta u_\eta^0 \Delta\eta\right)\Big|_w^e + \left(\frac{\Gamma}{J}\beta u_\xi^0 \Delta\xi\right)\Big|_s^n\right] \tag{37a}$$

$$b_P^{0v} = SJ\Delta\xi\Delta\eta - \left[\left(\frac{\Gamma}{J}\beta v_\eta^0 \Delta\eta\right)\Big|_w^e + \left(\frac{\Gamma}{J}\beta v_\xi^0 \Delta\xi\right)\Big|_s^n\right] \tag{37b}$$

$$B_{uP}^0 = \frac{\alpha_u B_P^u}{(A_P^{0u})_P} = \frac{\alpha_u (y_\eta)_P \Delta\xi\Delta\eta}{(A_P^{0u})_P} \tag{38a}$$

$$C_{uP}^0 = \frac{\alpha_u C_P^u}{(A_P^{0u})_P} = -\frac{\alpha_u (y_\xi)_P \Delta\xi\Delta\eta}{(A_P^{0u})_P} \tag{38b}$$

$$B_{vP}^0 = \frac{\alpha_v B_P^v}{(A_P^{0v})_P} = -\frac{\alpha_v (x_\eta)_P \Delta\xi\Delta\eta}{(A_P^{0v})_P} \tag{38c}$$

$$C_{vP}^0 = \frac{\alpha_v C_P^v}{(A_P^{0v})_P} = \frac{\alpha_v (x_\xi)_P \Delta\xi\Delta\eta}{(A_P^{0v})_P} \tag{38d}$$

In the above equations, the superscript 0 means that the values are obtained from the previous iteration. The grid velocities obtained from Equations (35a) and (35b) belong to the previous

DOI: 10.1002/fld

iteration. By mimicking these two equations, the following equations can be written for the corresponding interfacial velocities:

$$u_e^0 = \widehat{u_e^0} - \left(B_u^0 \frac{\partial p}{\partial \xi}\right)_e - \left(C_u^0 \frac{\partial p}{\partial \eta}\right)_e + (1-\alpha_u)u_e^0 \tag{39a}$$

$$v_e^0 = \widehat{v_e^0} - \left(B_v^0 \frac{\partial p}{\partial \xi}\right)_e - \left(C_v^0 \frac{\partial p}{\partial \eta}\right)_e + (1-\alpha_v)v_e^0 \tag{39b}$$

$$u_n^0 = \widehat{u_n^0} - \left(B_u^0 \frac{\partial p}{\partial \xi}\right)_n - \left(C_u^0 \frac{\partial p}{\partial \eta}\right)_n + (1-\alpha_u)u_n^0 \tag{39c}$$

$$v_n^0 = \widehat{v_n} - \left(B_v^0 \frac{\partial p}{\partial \xi}\right)_n - \left(C_v^0 \frac{\partial p}{\partial \eta}\right)_n + (1-\alpha_v)v_n^0 \tag{39d}$$

where

$$(B_u^0)_e = \frac{\alpha_u (y_\eta)_e (\delta\xi)_e \Delta\eta}{(A_P^{0u})_e}, \quad (C_u^0)_e = -\frac{\alpha_u (y_\xi)_e (\delta\xi)_e \Delta\eta}{(A_P^{0u})_e} \tag{40a}$$

$$(B_v^0)_e = -\frac{\alpha_v (x_\eta)_e (\delta\xi)_e \Delta\eta}{(A_P^{0v})_e}, \quad (C_v^0)_e = \frac{\alpha_v (x_\xi)_e (\delta\xi)_e \Delta\eta}{(A_P^{0v})_e} \tag{40b}$$

$$(B_u^0)_n = \frac{\alpha_u (y_\eta)_n \Delta\xi (\delta\eta)_n}{(A_P^{0u})_n}, \quad (C_u^0)_n = -\frac{\alpha_u (y_\xi)_n \Delta\xi (\delta\eta)_n}{(A_P^{0u})_n} \tag{40c}$$

$$(B_v^0)_n = -\frac{\alpha_v (x_\eta)_n \Delta\xi (\delta\eta)_n}{(A_P^{0v})_n}, \quad (C_v^0)_n = \frac{\alpha_v (x_\xi)_n \Delta\xi (\delta\eta)_n}{(A_P^{0v})_n} \tag{40d}$$

The variables in the interface, $\widehat{u_e}$, $\widehat{v_e}$, $\widehat{u_n}$, $\widehat{v_n}$, $(A_P^u)_e$, $(A_P^v)_e$, $(A_P^u)_n$, $(A_P^v)_n$, are linearly interpolated from the points P, E, N:

$$(A_P^{0u})_e = \frac{(\delta\xi)_{e^-}}{(\delta\xi)_e}(A_P^{0u})_E + \frac{(\delta\xi)_{e^+}}{(\delta\xi)_e}(A_P^{0u})_P, \quad (A_P^{0v})_e = \frac{(\delta\xi)_{e^-}}{(\delta\xi)_e}(A_P^{0v})_E + \frac{(\delta\xi)_{e^+}}{(\delta\xi)_e}(A_P^{0v})_P \tag{41a}$$

$$(A_P^{0u})_n = \frac{(\delta\eta)_{n^-}}{(\delta\eta)_n}(A_P^{0u})_N + \frac{(\delta\eta)_{n^+}}{(\delta\eta)_n}(A_P^{0u})_P, \quad (A_P^{0v})_n = \frac{(\delta\eta)_{n^-}}{(\delta\eta)_n}(A_P^{0v})_N + \frac{(\delta\eta)_{n^+}}{(\delta\eta)_n}(A_P^{0v})_P \tag{41b}$$

$$\widehat{u_e^0} = \frac{(\delta\xi)_{e^-}}{(\delta\xi)_e}\widehat{u_E^0} + \frac{(\delta\xi)_{e^+}}{(\delta\xi)_e}\widehat{u_P^0}, \quad \widehat{v_e^0} = \frac{(\delta\xi)_{e^-}}{(\delta\xi)_e}\widehat{v_E^0} + \frac{(\delta\xi)_{e^+}}{(\delta\xi)_e}\widehat{v_P^0} \tag{42a}$$

$$\widehat{u_n^0} = \frac{(\delta\eta)_{n^-}}{(\delta\eta)_n}\widehat{u_N^0} + \frac{(\delta\eta)_{n^+}}{(\delta\eta)_n}\widehat{u_P^0}, \quad \widehat{v_n^0} = \frac{(\delta\eta)_{n^-}}{(\delta\eta)_n}\widehat{v_N^0} + \frac{(\delta\eta)_{n^+}}{(\delta\eta)_n}\widehat{v_P^0} \tag{42b}$$

Equations (39a), (39b) and (39c), (39d) are substituted into Equations (6a) and (6b) for the cell face contravariant velocities with the under-relaxation factor incorporated. Then the cell face

DOI: 10.1002/fld

contravariant velocities can be expressed as:

$$U_e = \left(\widehat{u^0}\frac{\partial y}{\partial \eta} - \widehat{v^0}\frac{\partial x}{\partial \eta}\right)_e - \left(B_f^{0u}\frac{\partial p}{\partial \xi}\right)_e + \left(C_f^{0u}\frac{\partial p^0}{\partial \eta}\right)_e + (1-\alpha_u)(y_\eta)_e u_e^0 - (1-\alpha_v)(x_\eta)_e v_e^0 \quad (43a)$$

$$V_n = \left(\widehat{v^0}\frac{\partial x}{\partial \xi} - \widehat{u^0}\frac{\partial y}{\partial \xi}\right)_n + \left(B_f^{0v}\frac{\partial p^0}{\partial \xi}\right)_n - \left(C_f^{0v}\frac{\partial p}{\partial \eta}\right)_n + (1-\alpha_v)(x_\xi)_n v_n^0 - (1-\alpha_n)(y_\xi)_n u_n^0 \quad (43b)$$

where

$$B_{fe}^{0u} = B_{ue}^0 y_\eta - B_{ve}^0 x_\eta = \left(\frac{\alpha_u y_\eta^2}{A_p^{0u}} + \frac{\alpha_v x_\eta^2}{A_p^{0v}}\right)_e (\delta\xi)_e \Delta\eta \quad (44a)$$

$$C_{fe}^{0u} = -C_{ue}^0 y_\eta + C_{ve}^0 x_\eta = \left(\frac{\alpha_u y_\xi y_\eta}{A_p^{0u}} + \frac{\alpha_v x_\xi x_\eta}{A_p^{0v}}\right)_e (\delta\xi)_e \Delta\eta \quad (44b)$$

$$B_{fn}^{0v} = -B_{vn}^0 x_\xi + B_{un}^0 y_\xi = \left(\frac{\alpha_v y_\xi y_\eta}{A_p^{0u}} + \frac{\alpha_n x_\xi x_\eta}{A_p^{0v}}\right)_n (\delta\eta)_n \Delta\xi \quad (45a)$$

$$C_{fn}^{0v} = C_{vn}^0 x_\xi - C_{un}^0 y_\xi = \left(\frac{\alpha_v y_\xi^2}{A_p^{0u}} + \frac{\alpha_u x_\xi^2}{A_p^{0v}}\right)_n (\delta\eta)_n \Delta\xi \quad (45b)$$

For the convenience to account for the presence of the velocity under-relaxation factor the under-relaxation factor for u and v momentum equations are assumed to be the same, and for most flow computations in the previous literature this is often the case.

Under the condition of $\alpha_u = \alpha_v = \alpha$ Equations (43a) and (43b) can be rewritten as

$$U_e = \left(\widehat{u^0}\frac{\partial y}{\partial \eta} - \widehat{v^0}\frac{\partial x}{\partial \eta}\right)_e - \left(B_f^{0u}\frac{\partial p}{\partial \xi}\right)_e + \left(C_f^{0u}\frac{\partial p^0}{\partial \eta}\right)_e + (1-\alpha)U_e^0 \quad (46a)$$

$$V_n = \left(\widehat{v^0}\frac{\partial x}{\partial \xi} - \widehat{u^0}\frac{\partial y}{\partial \xi}\right)_n + \left(B_f^{0v}\frac{\partial p^0}{\partial \xi}\right)_n - \left(C_f^{0v}\frac{\partial p}{\partial \eta}\right)_n + (1-\alpha)V_n^0 \quad (46b)$$

The coefficients B_{fe}^{0u}, C_{fe}^{0u}, B_{fn}^{0v}, C_{fn}^{0v} are recast as:

$$B_{fe}^{0u} = B_{ue}^0 y_\eta - B_{ve}^0 x_\eta = \left(\frac{y_\eta^2}{A_p^{0u}} + \frac{x_\eta^2}{A_p^{0v}}\right)_e \alpha(\delta\xi)_e \Delta\eta \quad (47a)$$

$$C_{fe}^{0u} = -C_{ue}^0 y_\eta + C_{ve}^0 x_\eta = \left(\frac{y_\xi y_\eta}{A_p^{0u}} + \frac{x_\xi x_\eta}{A_p^{0v}}\right)_e \alpha(\delta\xi)_e \Delta\eta \quad (47b)$$

DOI: 10.1002/fld

$$B_{fn}^{0v} = -B_{vn}^{0} x_\xi + B_{un}^{0} y_\xi = \left(\frac{y_\xi y_\eta}{A_p^{0u}} + \frac{x_\xi x_\eta}{A_p^{0v}} \right)_n \alpha(\delta\eta)_n \Delta\xi \tag{48a}$$

$$C_{fn}^{0v} = C_{vn}^{0} x_\xi - C_{un}^{0} y_\xi = \left(\frac{y_\xi^2}{A_p^{0u}} + \frac{x_\xi^2}{A_p^{0v}} \right)_n \alpha(\delta\eta)_n \Delta\xi \tag{48b}$$

When the iteration converges, U_e and U_e^0 reach the same value. From Equations (46a), (46b) it can be observed that the effect of the under-relaxation factor is fully eliminated.

Defining the pseudo-cell face contravariant velocities as follows:

$$\widehat{U_e^0} = \left(\widehat{u^0} \frac{\partial y}{\partial \eta} - \widehat{v^0} \frac{\partial x}{\partial \eta} \right)_e + \left(C_f^{0u} \frac{\partial p}{\partial \eta} \right)_e + (1-\alpha) U_e^0 \tag{49a}$$

$$\widehat{V_n^0} = \left(\widehat{v^0} \frac{\partial x}{\partial \xi} - \widehat{u^0} \frac{\partial y}{\partial \xi} \right)_n + \left(B_f^{0v} \frac{\partial p}{\partial \xi} \right)_n + (1-\alpha) V_n^0 \tag{49b}$$

Then Equations (46a) and (46b) can be rewritten as

$$U_e = \widehat{U_e^0} - \left(B_f^{0u} \frac{\partial p}{\partial \xi} \right)_e \tag{50a}$$

$$V_n = \widehat{V_n^0} - \left(C_f^{0v} \frac{\partial p}{\partial \eta} \right)_n \tag{50b}$$

Equations (50a) and (50b) are substituted into the continuity equation, then the pressure equation in the predictor step is obtained:

$$A_P^0 p_P^* = \sum A_{\mathrm{nb}}^0 p_{\mathrm{nb}}^* + b \tag{51}$$

where

$$A_P^0 = A_E^0 + A_W^0 + A_N^0 + A_S^0 \tag{52a}$$

$$(A_E^0)_P = (A_W^0)_E = \left(\frac{\rho \Delta\eta B_f^{0u}}{\delta\varsigma} \right)_e \tag{52b}$$

$$(A_N^0)_P = (A_S^0)_N = \left(\frac{\rho \Delta\xi C_f^{0v}}{\delta\eta} \right)_n \tag{52c}$$

$$b = (\rho \Delta\eta \widehat{U^0})|_e^w + (\rho \Delta\xi \widehat{V^0})|_n^s \tag{52d}$$

To further improve the robustness of the algorithm, a pressure under-relaxation factor is introduced. The final form of pressure in the predictor step can be expressed as

$$\frac{A_P^0}{\alpha_p} p_P^* = \sum A_{\mathrm{nb}}^0 p_{\mathrm{nb}}^* + b + \frac{1-\alpha_p}{\alpha_p} A_P^0 p_P^0 \tag{53}$$

DOI: 10.1002/fld

Intermediate step of extended CLEAR algorithm

The pressure which is solved from the pressure equation (53) is taken as the source term of momentum equation and the intermediate Cartesian velocities u_p^*, v_p^* are obtained after solving the momentum equations. Then interface contravariant velocities are updated using the solved Cartesian velocities at the nodes. In the CLEAR algorithm, the calculation of interface contravariant velocities is different from the SIMPLER algorithm and it does not use the additional pressure gradient term. By imitating Equations (36a) and (36b), under the condition of $\alpha_u = \alpha_v = \alpha \neq 1$, the intermediate pseudo-velocities at grid points can be expressed as

$$\widehat{u_P^i} = \frac{\sum A_{\mathrm{nb}}^{0u} u_{\mathrm{nb}}^* + b_P^{0u}}{(A_P^{0u})_P/\alpha} \tag{54a}$$

$$\widehat{v_P^i} = \frac{\sum A_{\mathrm{nb}}^{0v} v_{\mathrm{nb}}^* + b_P^{0v}}{(A_P^{0v})_P/\alpha} \tag{54b}$$

The superscript i stands for the Cartesian variable in the intermediate iteration. The corresponding interface Cartesian velocities are linearly interpolated as

$$\widehat{u_e^i} = \frac{(\delta\xi)_{e^-}}{(\delta\xi)_e}\widehat{u_E^i} + \frac{(\delta\xi)_{e^+}}{(\delta\xi)_e}\widehat{u_P^i}, \quad \widehat{v_e^i} = \frac{(\delta\xi)_{e^-}}{(\delta\xi)_e}\widehat{v_E^i} + \frac{(\delta\xi)_{e^+}}{(\delta\xi)_e}\widehat{v_P^i} \tag{55a}$$

$$\widehat{u_n^i} = \frac{(\delta\eta)_{n^-}}{(\delta\eta)_n}\widehat{u_N^i} + \frac{(\delta\eta)_{n^+}}{(\delta\eta)_n}\widehat{u_P^i}, \quad \widehat{v_n^i} = \frac{(\delta\eta)_{n^-}}{(\delta\eta)_n}\widehat{v_N^i} + \frac{(\delta\eta)_{n^+}}{(\delta\eta)_n}\widehat{v_P^i} \tag{55b}$$

From Equations (46a) and (46b), the intermediate interface contravariant velocities are expressed as

$$U_e^* = \left(\widehat{u^i}\frac{\partial y}{\partial \eta} - \widehat{v^i}\frac{\partial x}{\partial \eta}\right)_e - \left(B_f^{0u}\frac{\partial p^*}{\partial \xi}\right)_e + \left(C_f^{0u}\frac{\partial p^*}{\partial \eta}\right)_e + (1-\alpha)U_e^0 \tag{56a}$$

$$V_n^* = \left(\widehat{v^i}\frac{\partial x}{\partial \xi} - \widehat{u^i}\frac{\partial y}{\partial \xi}\right)_n + \left(B_f^{0v}\frac{\partial p^*}{\partial \xi}\right)_n - \left(C_f^{0v}\frac{\partial p^*}{\partial \eta}\right)_n + (1-\alpha)V_n^0 \tag{56b}$$

The coefficient B_f^{0u}, C_f^{0u}, B_f^{0v}, C_f^{0v} are calculated with Equations (58) and (59). It can be seen that in Equations (56a) and (56b) pressure difference of two adjacent grid points is introduced to prevent the possible oscillation of pressure field. When iteration converges, the value of U_e^0 is equal to that of U_e^*, thus the effect of the under-relaxation factor can be eliminated to make the intermediate contravariant velocity independent of the under-relaxation factor. Equations (56a) and (56b) can be regarded as an improved MIM for the interfacial velocities.

According to the idea of CLEAR algorithm on the staggered grid and orthogonal coordinates, the improved interfacial velocity obtained above is then used to re-calculate the coefficients of the momentum equations by Equations (16)–(18).

Corrector step of extended CLEAR algorithm

In this step, the improved pressure equation is derived. In order to derive this equation an appropriate expression for the improved interfacial controvariant velocity should be constructed. This interfacial velocity should possess the following features: (1) it does not omit the terms of the neighbouring

DOI: 10.1002/fld

grid points; (2) the cross pressure gradient terms should be included. As for the staggered grid system in orthogonal coordinates this improved interfacial controvariant velocity is expressed by the sum of two terms: an improved pseudo-interfacial velocity and a pressure gradient term. In order to calculate the improved pseudo-velocity, a second velocity relaxation factor, β, is introduced, and it is also assumed that $\beta_u = \beta_v = \beta$.

The improved pseudo-Cartesian velocities at nodes are expressed

$$\widehat{u_P^*} = \frac{\sum A_{\mathrm{nb}}^{*u} u_{\mathrm{nb}}^* + b_P^{*u}}{(A_P^{*u})_P/\beta}, \quad \widehat{v_P^*} = \frac{\sum A_{\mathrm{nb}}^{*v} v_{\mathrm{nb}}^* + b_P^{*v}}{(A_P^{*v})_P/\beta} \tag{57}$$

where

$$b_P^{*u} = SJ\Delta\xi\Delta\eta - \left[\left(\frac{\Gamma}{J}\beta u_\eta^*\Delta\eta\right)\Big|_w^e + \left(\frac{\Gamma}{J}\beta u_\xi^*\Delta\xi\right)\Big|_s^n\right] \tag{58}$$

$$b_P^{*v} = SJ\Delta\xi\Delta\eta - \left[\left(\frac{\Gamma}{J}\beta v_\eta^*\Delta\eta\right)\Big|_w^e + \left(\frac{\Gamma}{J}\beta v_\xi^*\Delta\xi\right)\Big|_s^n\right] \tag{59}$$

The momentum discretization coefficients A_{nb}^{*u}, A_{nb}^{*v} are the updated ones which are calculated based on the intermediate interface contravariant velocities U_e^*, V_n^*. The improved interface pseudo-Cartesian velocities can be interpolated from the neighbouring points:

$$\widehat{u_e^*} = \frac{(\delta\xi)_{e^-}}{(\delta\xi)_e}\widehat{u_E^*} + \frac{(\delta\xi)_{e^+}}{(\delta\xi)_e}\widehat{u_P^*}, \quad \widehat{v_e^*} = \frac{(\delta\xi)_{e^-}}{(\delta\xi)_e}\widehat{v_E^*} + \frac{(\delta\xi)_{e^+}}{(\delta\xi)_e}\widehat{v_P^*} \tag{60}$$

$$\widehat{u_n^*} = \frac{(\delta\eta)_{n^-}}{(\delta\eta)_n}\widehat{u_N^i} + \frac{(\delta\eta)_{n^+}}{(\delta\eta)_n}\widehat{u_P^*}, \quad \widehat{v_n^*} = \frac{(\delta\eta)_{n^-}}{(\delta\eta)_n}\widehat{v_N^*} + \frac{(\delta\eta)_{n^+}}{(\delta\eta)_n}\widehat{v_P^*} \tag{61}$$

Similar to Equations (49a) and (49b), the improved cell face contravariant pseudo-velocities are the defined as

$$\widehat{U_e^*} = \left(\widehat{u^*}\frac{\partial y}{\partial\eta} - \widehat{v^*}\frac{\partial x}{\partial\eta}\right)_e + \left(C_{fe}^{*u}\frac{\partial p^*}{\partial\eta}\right)_e + (1-\beta)U_e^* \tag{62a}$$

$$\widehat{V_n^*} = \left(\widehat{v^*}\frac{\partial x}{\partial\xi} - \widehat{u^*}\frac{\partial y}{\partial\xi}\right)_n + \left(B_{fn}^{*v}\frac{\partial p^*}{\partial\xi}\right)_n + (1-\beta)V_n^* \tag{62b}$$

Then similar to Equations (49a) and (49b) the cell face contravariant velocities of the present iteration which will satisfy the continuity equation are expressed as

$$U_e = \widehat{U_e^*} - \left(B_{fe}^{*u}\frac{\partial p}{\partial\xi}\right)_e \tag{63a}$$

$$V_n = \widehat{V_n^*} - \left(C_{fn}^{*v}\frac{\partial p}{\partial\eta}\right)_n \tag{63b}$$

DOI: 10.1002/fld

where

$$B_{fe}^{*u} = \left(\frac{y_\eta^2}{A_p^{*u}} + \frac{x_\eta^2}{A_p^{*v}} \right)_e \beta(\delta\xi)_e \Delta\eta \tag{64a}$$

$$C_{fe}^{*u} = \left(\frac{y_\xi y_\eta}{A_p^{*u}} + \frac{x_\xi x_\eta}{A_p^{*v}} \right)_e \beta(\delta\xi)_e \Delta\eta \tag{64b}$$

$$B_{fn}^{*v} = \left(\frac{y_\xi y_\eta}{A_p^{*u}} + \frac{x_\xi x_\eta}{A_p^{*v}} \right)_n \beta(\delta\eta)_n \Delta\xi \tag{65a}$$

$$C_{fn}^{*v} = \left(\frac{y_\xi^2}{A_p^{*u}} + \frac{x_\xi^2}{A_p^{*v}} \right)_n \beta(\delta\eta)_n \Delta\xi \tag{65b}$$

It can be observed that a $1-\delta$ pressure difference is introduced in the solution process for the second time that will further damp out the false pressure distribution. It can also be seen that when iteration converges, the U_e equals to U_e^*, and the converged solution is also independent of the second relaxation factor.

The main node velocities are improved in the following equations:

$$u_P = \widehat{u_P^*} - B_{uP}^* \left(\frac{\partial p}{\partial \xi} \right)_P - C_{uP}^* \left(\frac{\partial p^*}{\partial \eta} \right)_P + (1-\beta) u_p^* \tag{66a}$$

$$v_P = \widehat{v_P^*} - B_{vP}^* \left(\frac{\partial p^*}{\partial \xi} \right)_P - C_{vP}^* \left(\frac{\partial p}{\partial \eta} \right)_P + (1-\beta) v_p^* \tag{66b}$$

According to our numerical practice the value of second relaxation factor β is related to velocity under-relaxation factor α as

$$\beta = \begin{cases} 0.5, & 0 \leqslant \alpha \leqslant 0.5 \\ 1, & 0.5 \leqslant \alpha \leqslant 1 \end{cases} \tag{67}$$

As indicated in Reference [16], when the velocity under-relaxation factor is almost approaching 1, the second relaxation factor β can be greater than one.

Equations (63a) and (63b) are substituted into the continuity equation to gain the improved pressure which makes the contravariant velocity satisfy the continuity equation. The improved pressure equation is then obtained as

$$A_P^* p_P = \sum A_{\mathrm{nb}}^* p_{\mathrm{nb}} + b \tag{68}$$

where

$$A_P^* = A_E^* + A_W^* + A_N^* + A_S^* \tag{69}$$

$$(A_E^*)_P = (A_W^*)_E = \left(\frac{\rho \Delta\eta B_f^{*u}}{\delta x} \right)_e \tag{70}$$

DOI: 10.1002/fld

$$(A_N^*)_P = (A_S^*)_N = \left(\frac{\rho\Delta\xi C_f^{*v}}{\delta\eta}\right)_n \tag{71}$$

$$b = (\rho\Delta\eta\widehat{U^*})|_e^w + (\rho\Delta\xi\widehat{V^*})|_n^s \tag{72}$$

It can be seen that in the derivation of the improved pressure equation, Equation (68), no terms as terms $\sum A_{\mathrm{nb}}^{0u} u'_{\mathrm{nb}}$ and $\sum A_{\mathrm{nb}}^{0v} v'_{\mathrm{nb}}$ in Equations (24a) and (24b) are neglected, and it is this important feature that makes the present algorithm fully implicit. In addition, unlike the extended SIMPLER algorithm proposed in Reference [19] where an additional pressure gradient term was added in the updated interfacial contravariant velocity (see Equations (24a), (24b)), no extra term was added. This makes the mass conservation law being strictly satisfied.

To improve the robustness of the CLEAR algorithm, the pressure under-relaxation factor is also incorporated into the improved pressure equation. Then the final improved pressure equation is expressed as

$$\frac{A_P}{\alpha_P} p_P = \sum A_{\mathrm{nb}} p_{\mathrm{nb}} + b + \frac{1-\alpha_P}{\alpha_P} A_P p_p^* \tag{73}$$

Calculation procedure of extended CLEAR algorithm

The calculation procedure of extended CLEAR algorithm can be summarized as follows:

(1) Assume the initial velocity field u_P^0, v_P^0, U_f^0, V_f^0.
(2) Based on the interface contravariant velocity and Cartesian velocity at the nodes, calculate the coefficient of the momentum equation and interface pseudo-contravariant velocity $\widehat{U_e^0}$, Equation (49a), $\widehat{V_n^0}$, Equation (49b).
(3) Calculate the coefficients of pressure equation in the predictor step: B_{fe}^{0u}, C_{fn}^{0v}, Equations (47), (48).
(4) Solve the first pressure equation (53) and obtain the pressure field p^*.
(5) Based on the obtained pressure field solve momentum equations to gain the intermediate velocity value u_P^*, v_P^*.
(6) Calculate the intermediate interface contravariant U_e^*, Equation (56a), V_n^*, Equation (56b).
(7) Recalculating the momentum coefficients and improved interface pseudo-contravariant velocity $\widehat{U_e^*}$, Equation (62a) and $\widehat{V_n^*}$, Equation (62b).
(8) Calculate the coefficients of the improved pressure equation B_{fe}^{*u}, Equation (64a), C_{fn}^{*v}, Equation (64b).
(9) Solve the second pressure equation, Equation (85), to gain the improved pressure p.
(10) Calculate the present contravariant velocity U_e, Equation (63a) and V_n, Equation (63b), and Cartesian velocity at nodes as follows.
(11) Calculate the coefficients of other general variable and solve the related discretized equation.
(12) Return to step 2 and repeat until convergence is reached.

APPLICATIONS OF THE EXTENDED-CLEAR ALGORITHM

In this section, the above described extended CLEAR algorithm will first be applied to numerically solve the fluid flow and heat transfer problem between a concentric cylinder surrounded by a square

DOI: 10.1002/fld

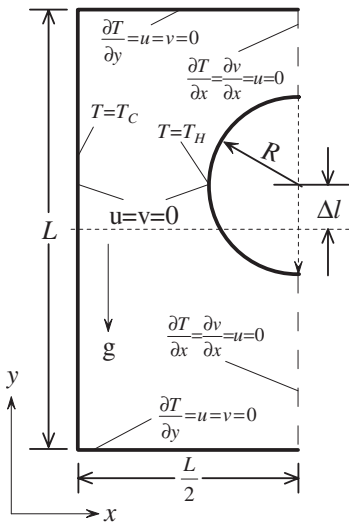

Figure 3. Concentric cylinder enclosed in a square duct.

duct (problem 1). This is a typical problem proposed in Reference [31] to examine the feasibility of numerical methods solving flow field in an irregular domain with non-staggered grid system. The physical problem is sketched in Figure 3, where only the left half geometry has been shown because of the symmetry condition. The side length of the outer square duct is L, the radius of the inner tube $R = 0.2L$ and the cylinder centre is displaced from the duct centre vertically for $\Delta l = 0.1L$. The temperature of the cylinder is maintained at constant value $T_H = 1$ and the vertical walls are kept at a lower temperature $T_C = 0$. The other boundary conditions are shown in Figure 3. The natural convection in the irregular enclosure is numerically simulated which is characterized by Prandtl number and the Ra number defined as

$$Ra = \rho^2 g \alpha L^3 (T_H - T_C) Pr/\eta^2 \tag{74}$$

The calculation is conducted with $Ra = 10^6$, $Pr = 10$ so as to compare with Reference [31]. The grid meshes is 102×102 which is schematically depicted in Figure 4, with much less grid lines for the convenience of presentation. The predicted stream lines and temperature contour lines using CLEAR algorithm are compared with the results in Reference [31] and are illustrated in Figures 5 and 6, respectively. It can be seen that the present predicted results are in good agreement with those presented in Reference [31]. Although the grid mesh number is more sparser than this paper, but the multi-grid technician is applied.

We study the iteration number under various under-relaxation factors to investigate the robustness of the extended algorithm. The variation of iteration number with under-relaxation factor is presented in Figure 7. It is revealed that the CLEAR can obtain converged solution under a wide range of under-relaxation factor ranging from 0.2 to 0.8. This confirms the good robustness characteristic of CLEAR algorithm.

After the reliability verification of the extended CLEAR algorithm, attention is now turned to the three issues set up in the above presentation for the numerical solution in a curvilinear coordinated with collocated grid system. That is the under-relaxation dependence of solution, the

DOI: 10.1002/fld

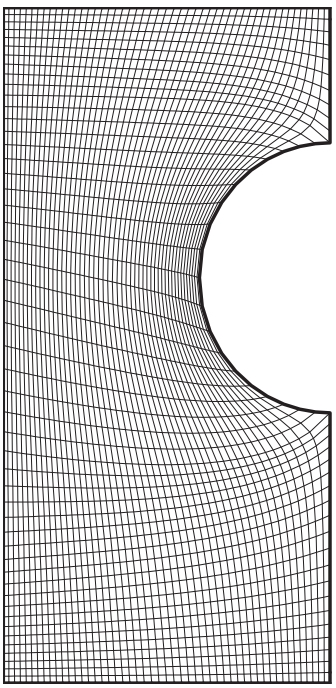

Figure 4. The generated grid of problem 1.

robustness of the algorithm and the possible oscillation of pressure fields at small value of velocity under-relaxation factor. The flow field prediction in the lid-driven cavity with inclined side walls (Figure 8) is taken as a typical problem (problem 2) to examine the above behaviour. This test problem is also proposed in Reference [31] to examine the major features of an algorithm in the non-orthogonal curvilinear coordinates.

The computations by the extended CLEAR algorithm were performed for the inclined angles of 45° and 30° and 5°. The simulation is conducted for *Re* number of 1000, and the adopted meshes is 103×103 for 45°, 30° and 83×83 for 5°.

The *Re* number is defined as

$$Re = \frac{\rho \cdot u_L \cdot L}{\eta} \tag{75}$$

The convergence criteria is that the non-dimensional maximum mass conservation residue of control volumes is smaller than 5×10^{-8}, which is defined as

$$\mathrm{RS}_{\max} = \frac{(\rho \Delta \eta U_f^*)|_e^w + (\rho \Delta \xi V_f^*)|_n^s}{\mathrm{Flow}_{\mathrm{ch}}} \tag{76}$$

where $\mathrm{Flow}_{\mathrm{ch}}$ is the characteristic flow rate which is defined as the sum of absolute mass flow rate along the CL1 section.

$$\mathrm{Flow}_{\mathrm{ch}} = \sum \rho |U_f| \Delta y_j \tag{77}$$

DOI: 10.1002/fld

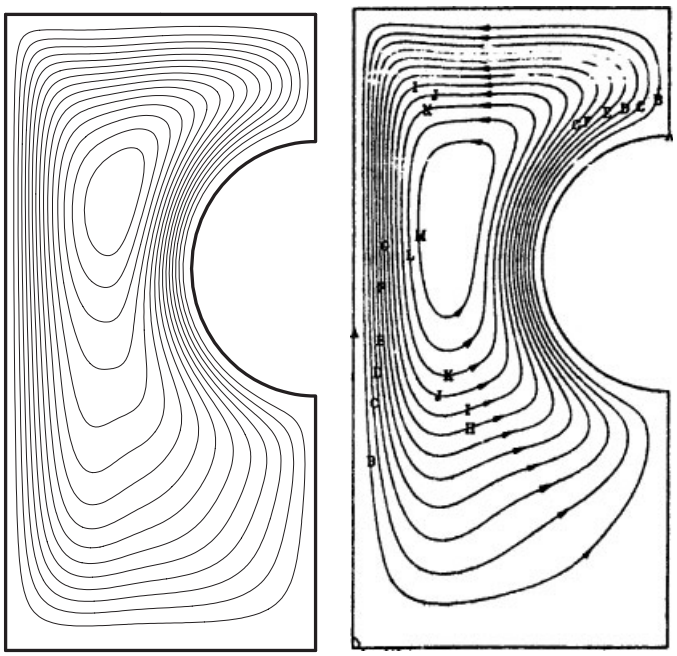

Figure 5. The stream function comparison for problem 1: (a) results of CLEAR algorithm; and (b) results of Reference [31].

The computational mesh is generated with a grid generation method based on solving Poisson equation [30]. To clearly show the grids, a coarse mesh is shown in Figure 9. It can be observed that when the inclination angle is 5°, the grid lines of two coordinates look like parallel. The predicted stream function for 45° and 30° are compared with the results in Reference [31] and presented in Figures 10 and 11, respectively. It can be seen that the two results are in good agreement. The predicted stream function with inclination angle of 5° is shown in Figure 12. Similar to the results of 45° and 30°, there are three primary vortex in the cavity and such results have not been reported in Reference [31], where the pressure correction equation of 5-point computational molecule was adopted.

To investigate the effect of the under-relaxation factor on the converged solution, the typical value of velocities of u and v in the locations in CL1 section with y coordinate being $0.45\sqrt{2}L$ under various under-relaxation factor are shown in Table III for angle of 45°. It is obvious that the converged velocity solution is independent of the under-relaxation factor.

The robustness of the extended CLEAR can also be verified by examining the variation range of the velocity under-relaxation factor with which converged solutions can be obtained. For the three inclined angles studied such examination results are presented in Figures 13–15, respectively. The good robustness of the extended CLEAR algorithm is thus illustrated. The major reason which can account for such good robustness of the extended CLEAR is that in the improved pressure equation in the extended CLEAR algorithm 5-point computational molecule is still used; however, the effects of neighbouring points and non-orthogonal term were not dropped but treated explicitly by including the related terms into the improved interface pseudo-contravariant velocity.

DOI: 10.1002/fld

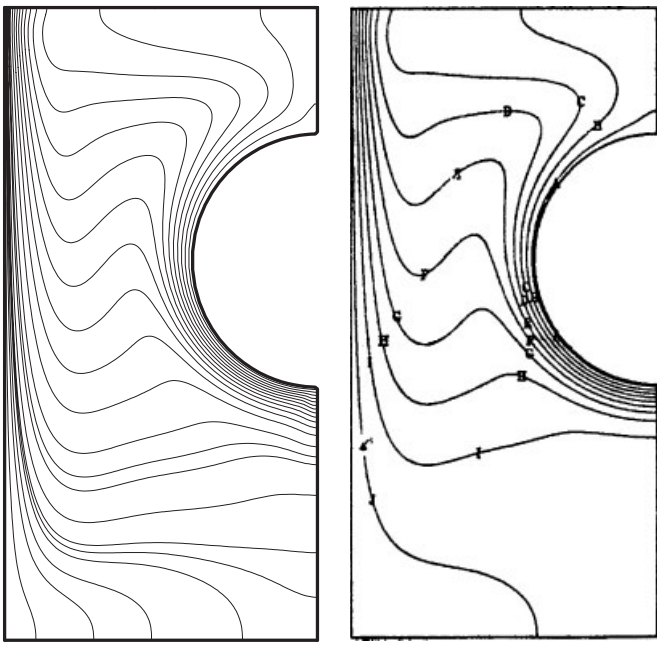

Figure 6. The temperature contour lines comparison for problem 1: (a) results of CLEAR algorithm; and (b) results of Reference [31].

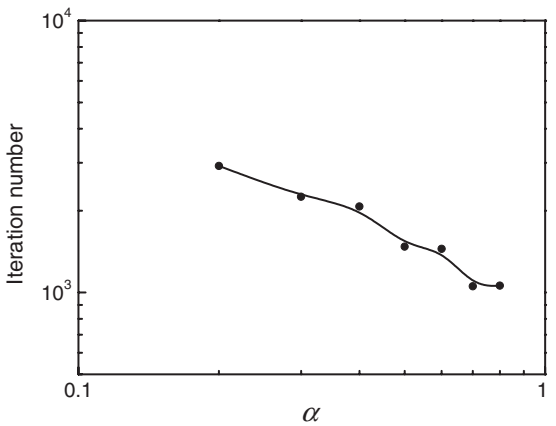

Figure 7. The variation of iteration number with under-relaxation factor for problem 1.

Finally to show the good coupling between velocity and pressure, computation was conducted for the inclined angle of 5° at the velocity under-relaxation factor of 0.2 and we still obtain a smooth profile of the pressure (see Figure 16 and Table IV), and no any oscillation in pressure is found.

DOI: 10.1002/fld

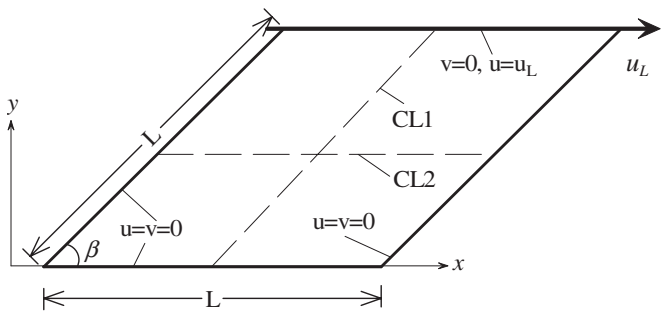

Figure 8. Computation domain and boundary conditions for problem 2.

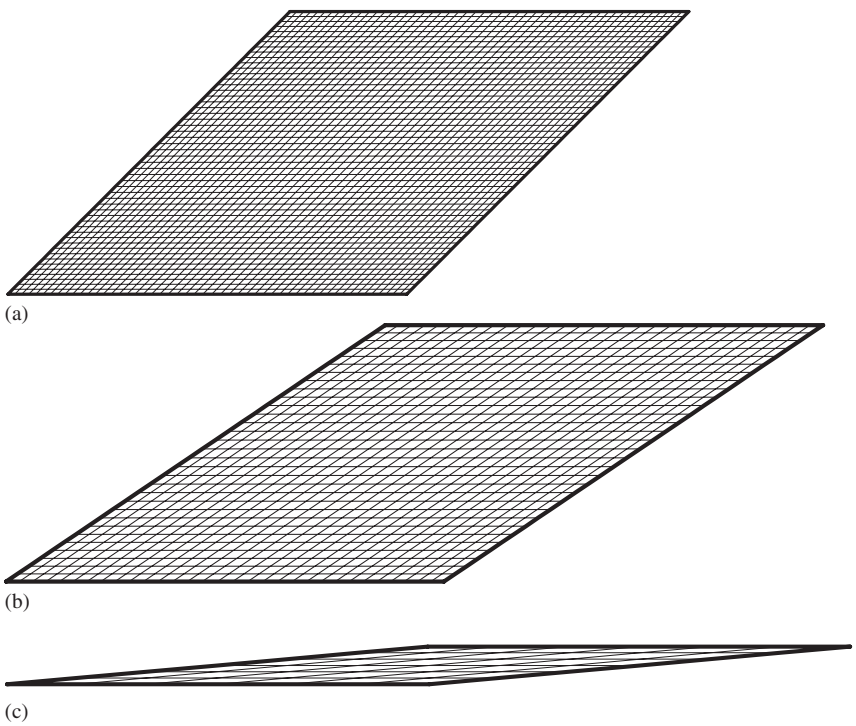

Figure 9. The generated grid for problem 2: (a) $\beta = 45°$; (b) $\beta = 30°$; and (c) $\beta = 5°$.

CONCLUSIONS

In this paper, the fully implicit algorithm for incompressible fluid flow, CLEAR, is successfully extended to the collocated grid system in non-orthogonal curvilinear coordinates. The solution-independency on the under-relaxation factor is guaranteed by an improved momentum interpolation of the interfacial contravariant velocity. The checkerboard pressure field is prevented by introducing

DOI: 10.1002/fld

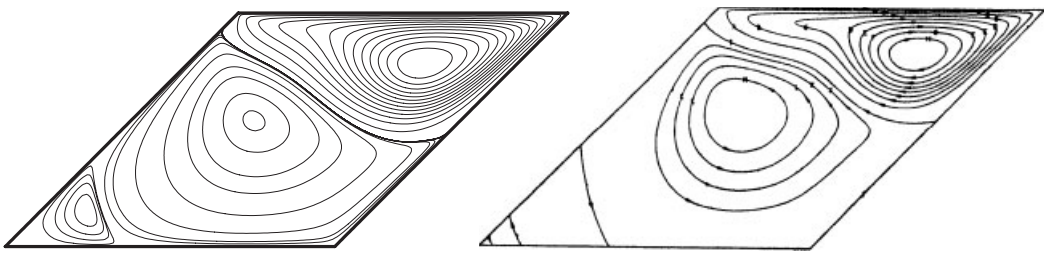

Figure 10. The stream function comparison ($\beta = 45°$): (a) results of CLEAR; and (b) results of Reference [31].

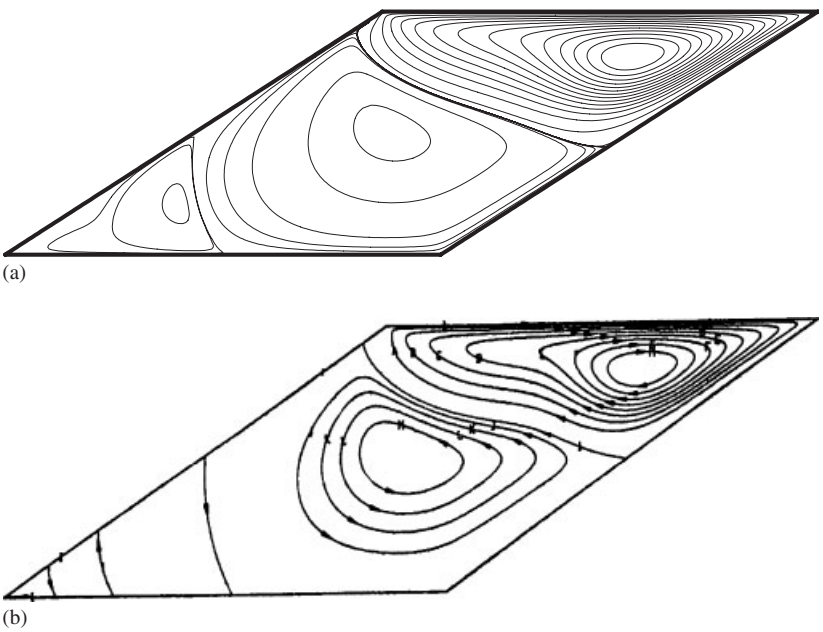

Figure 11. The stream function comparison ($\beta = 30°$): (a) results of CLEAR; and (b) results of Reference [31].

Figure 12. The predicted stream function of CLEAR algorithm ($\beta = 5°$).

the $(1 - \delta)$ pressure difference at the cell interface twice during the solution process. And the cross pressure gradient terms are all taken into account in a explicit way, so that the robustness of the algorithm is greatly enhanced. Numerical simulations conducted for the natural convection

DOI: 10.1002/fld

Table III. Velocity value with different under-relaxation factor ($\beta = 45°$).

	(α)					
Variable	0.2	0.3	0.4	0.5	0.6	0.7
u	0.50286	0.50289	0.50289	0.50294	0.50291	0.50295
v	−3.1326E-3	−3.1326E-3	−3.1326E-3	−3.1305E-3	−3.1326E-3	−3.1324E-3

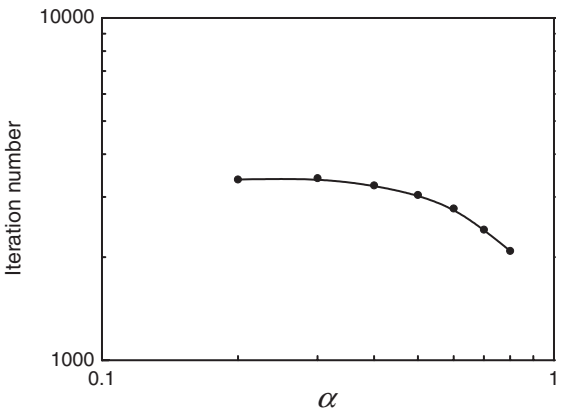

Figure 13. The variation of iteration number with under-relaxation factor ($\beta = 45°$).

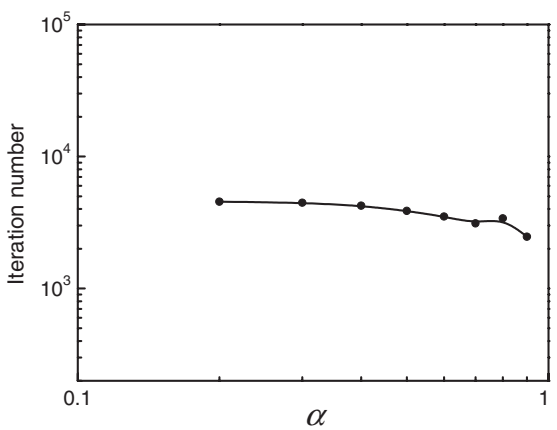

Figure 14. The variation of iteration number with under-relaxation factor ($\beta = 30°$).

in an irregular enclosure and flow in an inclined lid-driven cavity show good behaviour of the algorithm. For the lid-driven flow in inclined cavity, the pressure profile exhibit good smoothness at small under-relaxation factor (0.2) and converged solution can be obtained even at the inclined

DOI: 10.1002/fld

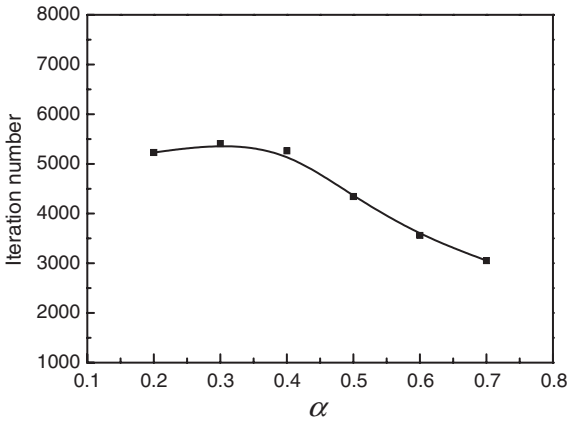

Figure 15. The variation of iteration number with under-relaxation factor ($\beta = 5°$).

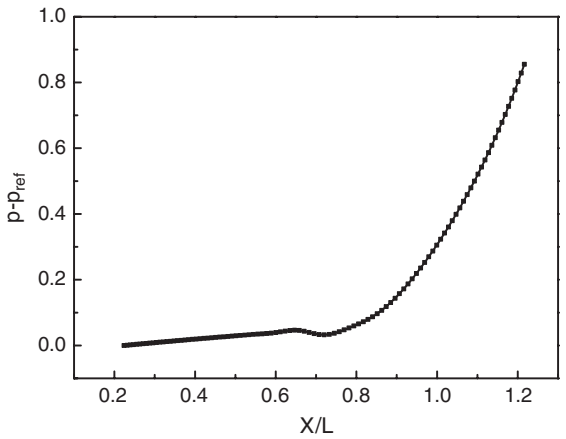

Figure 16. Pressure profile along the CL2 section ($\beta = 5°$, $\alpha = 0.2$).

Table IV. Some pressure distribution at $\alpha = 0.2$ of inclined angle 5°.

X/L	0.304	0.393	0.491	0.600	0.720	0.840	0.949	1.047	1.136	1.216
$p - p_{\text{ref}}$	0.009	0.019	0.028	0.039	0.032	0.087	0.219	0.399	0.609	0.855

angle as small as a 5° only with 5-point computational molecule, while the conventional extended SIMPLE-series algorithm can converge only when the inclined angle is equal to or larger than 30° under the same condition.

DOI: 10.1002/fld

NOMENCLATURE

A_P, A_E, A_W, A_N, A_S	coefficients in the discretized equation
A	surface area
B	source term
B	coefficients in pressure or pressure correction equation
C	coefficients in pressure or pressure correction equation
F	interpolation factor
F	flow rate
flow_{ch}	characteristic (reference) flow rate
J	Jacobi factor
L	length, m
P	pressure
p'	pressure correction
$\overline{p}_\xi$	the average value of pressure gradient in the ξ direction
$\overline{p}_\eta$	the average value of pressure gradient in the η direction
Pr	Prandtl number
Re	Reynolds number
RS_{MAX}	relative mass flow rate unbalance of control volume
U, v	velocity component in x, y direction
U', v'	velocity correction
$\widehat{u}, \widehat{v}$	pseudo-velocity
U, V	contravariant velocity
$\widehat{U}, \widehat{V}$	contravariant pseudo-velocity
$\overline{U}, \overline{V}$	contravariant velocity obtained by linear interpolation
U', V'	contravariant velocity correction
$\overrightarrow{U}$	mean contravariant velocity
U_{lid}	moving velocity of lid
X, y	coordinates in physical domain
X, Y	coordinates in computational domain
$x_\xi, x_\eta, y_\xi, y_\eta$	geometry factor

Greek letters

α	under-relaxation factor
Γ	nominal diffusion coefficient
ζ	coordinate in computational domain
η	coordinate in computational domain
μ	fluid dynamic viscosity
$\delta\xi, \delta\eta$	distance between two adjacent grid points in $x\zeta$ and η direction
$\Delta\xi, \Delta\eta$	distance between two adjacent face points in $x\zeta$ and η direction
ρ	fluid density
ϕ	general variable
δ	distance

DOI: 10.1002/fld

Subscripts

e, w, n, s	cell surface
Max	maximum
P, E, N, S, W	grid point
Nb	neighbouring points
Non	non-orthogonal term
u, v	refers to u, v momentum equation

Superscripts

$'$	correction
—	mean value
0	the previous iteration
i	intermediate value of Cartesian coordinates in iteration
$*$	intermediate value in iteration
$\rightarrow$	vector

ACKNOWLEDGEMENTS

The work reported here is supported by the National Natural Science Foundation of China (50476046, 50425620, 50576069) and the Basic Research Program of China (2006CB601203).

REFERENCES

1. Rhie CM, Chow WL. Numerical study of the turbulent flow past an airfoil with trading edge separations. *AIAA Journal* 1983; **21**(11):1525–1535.
2. Peric M, Kessler R, Scheuerer G. Comparison of finite volume methods with staggered and collocated grids. *Computer and Fluids* 1988; **16**:389–408.
3. Patankar SV, Spalding DB. A calculation procedure for heat mass and momentum transfer in three-dimensional parabolic flows. *International Journal of Heat and Mass Transfer* 1972; **15**:1787–1790.
4. Patankar SV. A calculation procedure for two-dimensional elliptic situations. *Numerical Heat Transfer* 1981; **4**:409–425.
5. van Doormaal JP, Raithby GD. Enhancement of SIMPLE method for predicting incompressible fluid flows. *Numerical Heat Transfer* 1984; **7**:147–163.
6. van Doormaal JP, Raithby GD. An evaluation of the segregated approach for predicting incompressible fluid flow. *ASME Paper 85-HT-9*, 1985.
7. Raithby GD, Schneider GE. Elliptic system: finite difference method. In *Handbook of Numerical Heat Transfer*, Minkowycz WJ, Sparrow EM, Pletcher RH, Schneider GE (eds). Wiley: New York, 1988; 241–289.
8. Issa RI. Solution of implicitly discretized fluid flow equation by operator-splitting. *Journal of Computational Physics* 1985; **62**:40–65.
9. Yen RH, Liu CH. Enhancement of the SIMPLER algorithm by an additional explicit corrector step. *Numerical Heat Transfer B* 1993; **24**:127–141.
10. Sheng Y, Shoukri M, Sheng G, Wood P. A modification to the SIMPLE method for buoyancy-driven flows. *Numerical Heat Transfer B* 1988; **33**:65–78.
11. Yu B, Ozoe H, Tao WQ. A modified pressure-correction scheme for the SIMPLER method, MSIMPLER. *Numerical Heat Transfer B* 2001; **39**:439–449.
12. Moukalled F, Darwish M. A unified formulation of the segregated class of algorithm for fluid flow at all speeds. *Numerical Heat Transfer B* 2000; **37**:103–139.
13. Patankar SV. *Numerical Heat Transfer and Fluid Flow*. Hemisphere Publishing Corporation: Washington, DC, 1980.

DOI: 10.1002/fld

14. Blosch E, Shyy W. The role of mass conservation in pressure-based algorithms. *Numerical Heat transfer B* 1993; **24**:415–429.
15. Shyy W, Mittal R. Solution methods for the incompressible Navier–Stokes equations. In *The Handbook of Fluid Dynamics*, Johnson RW (ed.). CRC Press: Johnson/Boca Raton, 1998; 1–31.33.
16. Tao WQ, Qu ZG, He YL. A novel segregated algorithm for incompressible fluid flow and hear transfer problems—CLEAR (Coupled & Linked Equations Algorithm Revised), Part 1: mathematical formulation and solution procedure. *Numerical Heat Transfer B* 2004; **45**:1–17.
17. Tao WQ, Qu ZG, He YL. A novel segregated algorithm for incompressible fluid flow and hear transfer problems—CLEAR (Coupled & Linked Equations Algorithm Revised), Part 2: application examples. *Numerical Heat Transfer B* 2004; **45**:19–48.
18. Qu ZG, Tao WQ, He YL. Implementation of CLEAR algorithm on collocated grid system and application examples. *Numerical Heat Transfer B* 2005; **47**(1):64–96.
19. Acharya S, Moukalled FH. Improvements to incompressible fluid flow calculation on a non-staggered curvilinear grid. *Numerical Heat Transfer B* 1999; **15**:131–152.
20. Parameswaran SS, Srinivasun A. Numerical aerodynamic simulation of steady and transient flows around two-dimensional bluff bodies using the nonstaggered grid system. *Numerical Heat Transfer A* 1992; **21**:443–461.
21. Shyy W, Vu TC. On the adoption of velocity variable grid system for fluid flow computation in curvilinear coordinates. *Journal of Computational Physics* 1991; **92**:82–105.
22. Majumdar S. Roles of under-relaxation in momentum interpolation for calculation of flow with non-staggered grids. *Numerical Heat Transfer* 1988; **13**:125–132.
23. Kobayashi MH, Pereira JCF. Calculation of incompressible laminar flows on a nonstaggered, nonorthogonal grid. *Numerical Heat Transfer B* 1991; **19**:343–362.
24. Miller TF, Schmidt FW. Use of a pressure–weighted interpolation method for the solution of incompressible Navier–Stokes equations on a non-staggered grid system. *Numerical Heat Transfer* 1988; **14**:213–233.
25. Kobayashi MH, Pereira JCF. Numerical comparison of momentum interpolation methods and pressure-velocity algorithm using nonstaggered grids. *Communications in Applied Numerical Methods* 1991; **7**:173–196.
26. Yu B, Tao W-Q, Wei J-J, Kawaguchi Y, Tagawa T, Ozoe H. Discussion on momentum interpolation method for collocated grids of incompressible flow. *Numerical Heat Transfer B* 2002; **42**:141–166.
27. Choi Sk, Nam HY, Cho M. Use of the momentum interpolation method for numerical solution of incompressible flows in complex geometries: choosing cell face velocities. *Numerical Heat Transfer B* 1993; **23**:21–41.
28. Peric PM. Analysis of pressure velocity coupling on nonorthogonal grids. *Numerical Heat Transfer B* 1999; **17**:63–82.
29. Yu B, Kawaguchi Y, Tao WQ, Ozoe H. Checkerboard pressure prediction due to the underrelaxation factor and time step size for a nonstaggered grid with momentum interpolation method. *Numerical Heat Transfer B* 2002; **41**:85–94.
30. Tao WQ. *Numerical Heat Transfer* (2nd edn). Xi'an Jiaotong University Press: Xi'an, 2001.
31. Peric DM. Finite volume method for prediction of fluid flow in arbitrarily shaped domains with moving boundaries. *International Journal for Numerical Methods in Fluids* 1990; **10**:771–790.

DOI: 10.1002/fld